

# Limited Reference, Reliable Generation: A Two-Component Framework for Tabular Data Generation in Low-Data Regimes

Mingxuan Jiang\*, Yongxin Wang\*, Ziyue Dai\*, Yicun Liu\*, Hongyi Nie<sup>†‡§</sup>, Sen Liu<sup>†§</sup>, Hongfeng Chai<sup>†</sup>

<sup>\*</sup>School of Computer Science, Fudan University, Shanghai, China

<sup>†</sup>Institute of Financial Technology, Fudan University, Shanghai, China

<sup>‡</sup>Northwestern Polytechnical University, Xi'an, China

{mxjiang24, yongxinwang24, zydai24, ycliu24}@m.fudan.edu.cn, hy\_nie@mail.nwpu.edu.cn, {senliu, hfchai}@fudan.edu.cn

**Abstract**—Synthetic tabular data generation is increasingly essential in data management, supporting downstream applications when real-world and high-quality tabular data is insufficient. Existing tabular generation approaches, such as generative adversarial networks (GANs), diffusion models, and fine-tuned Large Language Models (LLMs), typically require sufficient reference data, limiting their effectiveness in domain-specific databases with scarce records. While prompt-based LLMs offer flexibility without parameter tuning, they often fail to align the distribution of real data and cause localized redundancy in synthetic data, leading to degradation in downstream task performance. To overcome these issues, we propose *ReFine*, a framework that (i) derives symbolic *if-then* rules from interpretable models and embeds them into prompts to explicitly guide generation toward domain-specific feature distribution, and (ii) applies a dual-granularity filtering strategy that suppresses oversampling patterns and selectively refines rare but informative samples to reduce localized redundancy. Extensive experiments on various regression and classification benchmarks demonstrate that *ReFine* consistently outperforms state-of-the-art methods, achieving up to 0.44 absolute improvement in  $R^2$  for regression and 10.0% relative improvement in  $F_1$  for classification tasks.

**Index Terms**—Tabular Data Generation, Low-Data Regimes, Data Quality Filtering.

## I. INTRODUCTION

Tabular data, the core representation in database systems, underpins numerous data-driven machine learning applications, such as price prediction based on transaction databases in finance [1]–[4]. The performance of these models depends on the availability of large-scale, high-quality tabular datasets [5]. However, collecting such datasets is non-trivial due to issues such as high annotation costs and privacy concerns [6], [7]. Consequently, generating tabular data has gained growing traction in the database community as a promising alternative to mitigate those constraints [4], [8].

Previous mainstream methods for tabular data generation typically rely on non-language generative models such as variational autoencoders (VAE), diffusion models, and GANs

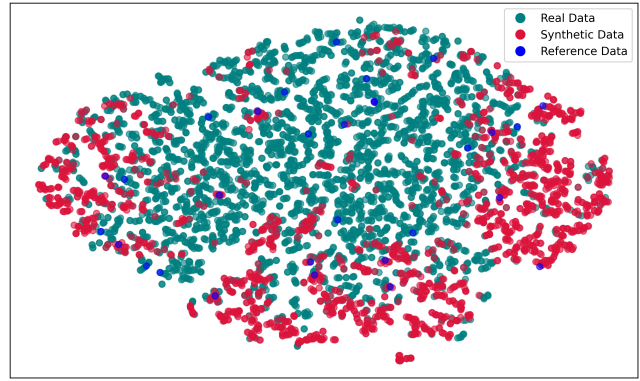


Fig. 1. Two key challenges in prompt-based LLM tabular data generation in low-data regimes: (i) **Distributional Drift**: LLMs often generate biased samples by relying on spurious correlations from pretraining rather than dataset-specific feature distribution. (ii) **Localized Redundancy**: Synthetic samples tend to concentrate in limited regions of the feature space due to repeated use of identical prompts.

[9]–[11]. Recently, LLMs have emerged as a promising alternative, leveraging their extensive pre-training knowledge to develop new approaches for tabular data generation [12]–[14]. Within the LLM-based paradigm, fine-tuning approaches have demonstrated notable success in aligning LLMs with tabular data formats and domain-specific patterns [15].

Both non-language generative models and LLM fine-tuning approaches share a fundamental prerequisite: access to sufficient *reference data*—the original labeled dataset used as the foundation for learning distributional patterns and generating new instances. In reality, many high-stakes fields have domain-specific databases with only a few dozen records (*i.e.*, *low-data regimes* [16]), such as rare disease records in healthcare or fraudulent transaction cases in finance [17], [18]. Under such conditions, the key prerequisite of sufficient reference data no longer holds, which prevents existing approaches from modeling feature dependencies and generating high-quality synthetic data [12], [19], [20]. Prompt-based LLM methods present an

<sup>§</sup> Corresponding authors.

attractive alternative by exploiting in-context learning without parameter modification, thereby reducing dependence on extensive reference data and avoiding overfitting when reference data are limited [16], [21]. However, prompt-based LLM tabular data generation methods face two challenges in low-data regimes (as shown in Fig. 1):

(i) **Distributional Drift**: Prompt-based methods rely heavily on LLMs’ pretrained knowledge, which may inadequately capture the specific statistical dependencies of the reference data [22]. This leads LLMs to favor spurious correlations from pretraining corpora over critical domain-specific feature correlations, resulting in synthetic samples that lack distributional realism [23], [24]. As shown in Fig. 1, when prompted with a limited number of reference data (**blue**), the LLM generates synthetic samples (**red**) that markedly deviate from the distributional support of real data (**cyan**). Many generated records appear in low-density or unsupported regions, underscoring the LLM’s inability to recover the target joint feature distribution from limited reference data alone, thereby compromising the fidelity of the synthesized data and the generalization of downstream models.

(ii) **Localized Redundancy**: Prompt-based generation conditions the LLM on the empirical distribution implied by the prompt itself [25], [26]. As a result, attribute combinations frequently observed in the reference records are regenerated disproportionately, while informative low-frequency patterns are rarely synthesized [27]. When tabular data must be produced in multiple batches due to output-length limitation, reusing the same prompt template further compounds this redundancy, causing synthetic samples to cluster around a narrow set of modes [16], [21]. As shown in Fig. 1, synthetic samples (**red**) form overly dense clusters in localized regions, in stark contrast to the broader and more balanced distribution of real data (**cyan**).

To systematically address the two key challenges of prompt-based tabular generation in low-data regimes, we propose **ReFine** (**R**ule-**G**uided **F**iltering), a framework comprising two components: rule-guided generation and post-generation distribution-based filtering. First, to accurately capture specific distribution often biased by LLMs in low-data regimes (Challenge i), we introduce **Rule-Guided Generation**, which extracts symbolic *if-then* rules from interpretable tree-based models. These rules are embedded into structured prompts to guide the LLM toward feature-label dependencies. Second, to correct sampling redundancy that persists despite prompt-based generation (Challenge ii), we propose **Dual-Granularity Filtering**. This component computes a Gini-based redundancy score to inform a two-level filtering process: chunk-level pruning of dominant high-frequency modes, and instance-level refinement to retain rare but informative samples. Our key contributions can be summarized as follows:

- We identify two key challenges of LLM in tabular data generation in low-data regimes: (i) *Distributional Drift* of synthetic data; and (ii) *Localized Redundancy* in synthetic data.

- To address the two challenges, we propose **ReFine**, a framework that constructs symbolic rules to guide tabular data generation, and applies proxy-based distribution estimation with dual-granularity filtering to correct sampling redundancy.
- Experimental results demonstrate that **ReFine** consistently outperforms state-of-the-art baselines across downstream tasks, achieving up to **0.44** absolute gain in  $R^2$  for regression and **10%** relative improvement in  $F1$  for classification. Comprehensive ablations further highlight the respective contributions of *Rule-Guided Generation* and *Dual-Granularity Filtering* components.

## II. RELATED WORK

### A. Non-LLM Tabular Generation Method

Early approaches to tabular data generation have primarily relied on non-language generative models such as GANs, variational autoencoder (VAE), and diffusion models. Specifically, CTGAN [9] adapts the GAN framework to tabular data by incorporating techniques for generating discrete variables, but requires extensive preprocessing to handle mixed data types and struggles when data is scarce. TabDDPM [10] employs diffusion processes to iteratively generate high-quality tabular data, particularly suitable for continuous variables. TABSYN [11] builds on the score-based generative model by extending diffusion to the VAE latent space and improving support for mixed-type data, and achieve excellent performance. While these methods differ in architecture, they all share a common limitation: a strong reliance on large-scale training data, which hinders their effectiveness in low-data regimes.

### B. LLM-based Tabular Generation Method

LLMs have recently gained attention for tabular data generation, particularly in domains like healthcare and finance where domain knowledge is essential. Unlike non-language models that learn only data distributions, LLMs can leverage rich pretrained knowledge, making them well-suited for structured data tasks. Based on how the LLM is used, these approaches can be broadly categorized into two groups: *fine-tuning methods* and *prompt-based methods*:

1) *Fine-Tuning Methods*: Fine-tuning methods adapt pre-trained LLMs to the structure of tabular data by updating LLM weights. This approach helps LLMs model feature dependencies and domain constraints for more coherent outputs. GReAT [15] is a foundational work, fine-tuning a pre-trained LLM on tabular data to generate tabular datasets. HARMONIC [28] fine-tunes LLMs using instructions derived from nearest-neighbor relationships, encouraging LLMs to learn inter-row patterns rather than memorizing records. Although fine-tuning enables high-fidelity generation with sufficient data, it is prone to severe overfitting in low-data regimes.

2) *Prompt-based Methods*: Prompt-based methods leverage the in-context learning ability of LLMs, enabling them to generate tabular data by conditioning on a few labeled examples embedded directly in the prompt. Without modifying model

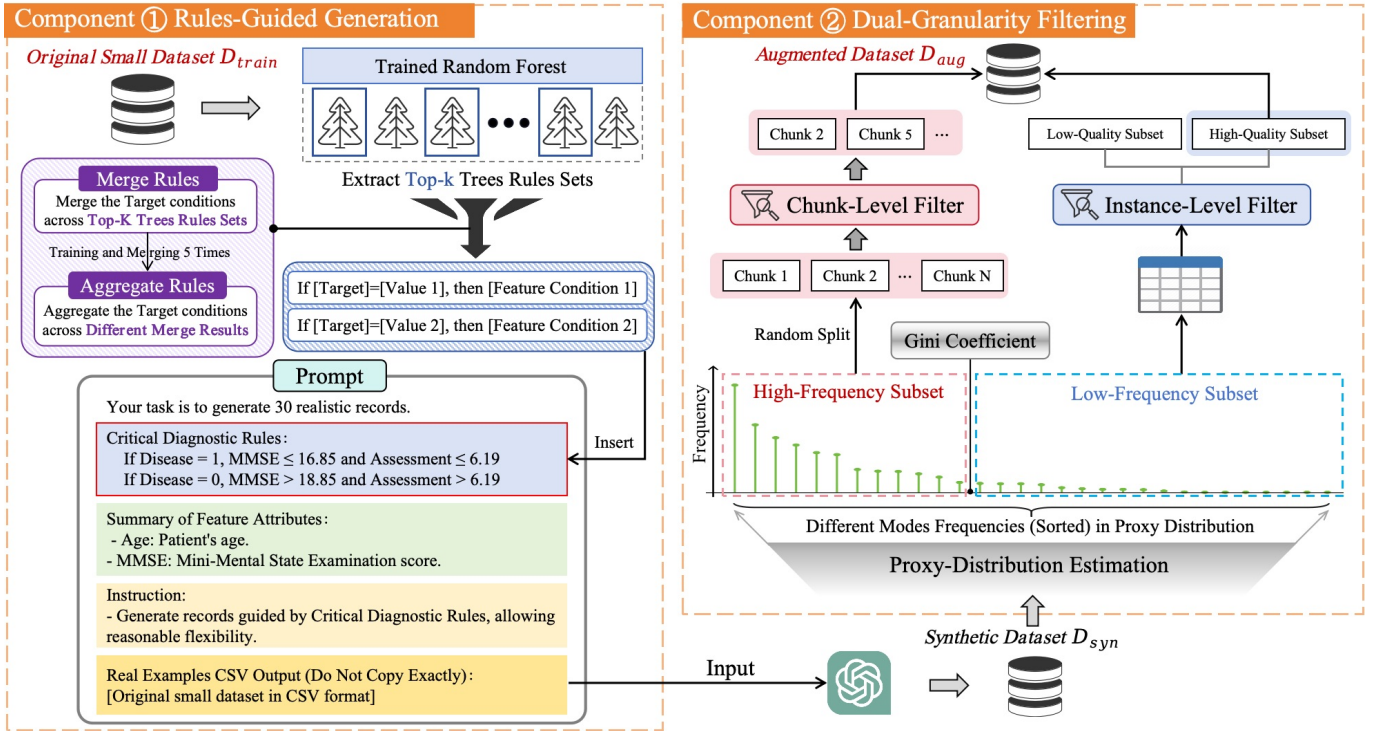


Fig. 2. Overall framework of **ReFine**, which consists of two components: (1) **Rule-Guided Generation**, which extracts clear feature dependencies from tree-based models and inserts them into prompts to guide LLM generation. (2) **Dual-Granularity Filtering** applies *chunk-level* suppression of high-frequency patterns and *instance-level* retention of low-frequency but informative samples, mitigating the localized redundancy caused by using identical prompts.

parameters, these methods use prompt design to guide the generation process. EPIC improves representation balance across classes by formatting grouped data and crafting class-aware prompts [21]. CLLM enhances data quality in low-resource scenarios by combining prompt design with a curation step that filters samples based on model confidence and uncertainty estimates [16]. However, prompt-based methods struggle to capture feature dependencies and often suffer from localized redundancy due to repeated use of identical prompts, limiting their effectiveness in low-data regimes.

### III. PROBLEM FORMULATION

We consider the problem of tabular data generation, with the goal of synthesizing data to improve the performance of downstream tasks in low-data regimes. Such low-data scenarios commonly arise in sensitive domains such as healthcare and finance [16], [17], [19], where only a few dozen labeled records are available. We define the tabular data generation problem in low-data regimes as follows.

**Definition 3.1: Tabular Data Generation in Low-data Regimes.** Let  $X \subseteq \mathbb{R}^d$  be the  $d$ -dimensional feature space and  $Y$  the label space (discrete for classification, real-valued for regression). Let  $D_{\text{train}} = \{(x_i, y_i)\}_{i=1}^N$  be a small labeled dataset independently and identically drawn from the unknown real distribution  $p_R(X, Y)$ , where  $x_i \in X$  and  $y_i \in Y$ , with  $N$  limited to only a few examples.

The task output is to define a generation function  $\mathcal{G}$  that maps  $D_{\text{train}}$  to a synthetic dataset:

$$D_{\text{syn}} = \mathcal{G}(D_{\text{train}}) = \{(\tilde{x}_j, \tilde{y}_j)\}_{j=1}^M.$$

where  $(\tilde{x}_j, \tilde{y}_j)$  is a synthetic sample, and  $M$  is the number of synthetic samples, typically satisfying  $M \gg N$ .

The task goal is to generate  $D_{\text{syn}}$  such that a model trained on it achieves strong predictive performance when evaluated on a held-out real test set  $D_{\text{test}} \sim p_R$ .

### IV. PROPOSED METHOD

In low-data regimes, prompt-based tabular data generation faces two persistent challenges: (1) **Distributional Drift**: LLMs tend to overlook dataset-specific distribution and instead rely on spurious correlations learned during pretraining. (2) **Localized Redundancy**: Due to prompt reuse across batches, LLMs tend to replicate high-frequency patterns while undersampling rare regions, leading to redundant samples in synthetic data.

To jointly address these challenges, we propose **ReFine**, a two-component framework that combines structural guidance during generation with distributional calibration after generation. As illustrated in Fig. 2, it includes: (1) **Rule-Guided Generation** extracts clear feature dependencies from tree-based models, serving as a bridge between the feature distribution of reference data  $D_{\text{train}}$  and LLM-based generation. These rules guide the LLM toward generating samples that more accurately reflect underlying feature-label dependencies from

### Aggregation Logic Prompt

Step 1: Identify Stable Rule Patterns

- Review all five rule sets for each label.
- Retain conditions or intervals that appear consistently ( $\geq 3$  out of 5).

Step 2: Generate Final Integrated Rules

- Create one rule per label using consensus intervals:

If [Target] = [Label], then [Condition 1] and [Condition 2]...

- Use proper operators ( $>$ ,  $\geq$ ,  $<$ ,  $\leq$ ); avoid overly broad intervals.
- Ensure clarity and consistency across rules.

### Merging Logic Prompt

- Collect all rules associated with the same [Target].

- For each feature, extract all related conditions across rules.

- Merge overlapping or adjacent intervals by:

1. Preserving class distinctions -- ensure boundaries between different target values remain clear.

2. Maximizing generalization -- merge similar ranges where possible, as long as they don't blur class separation.

Fig. 3. Structured prompts used in the rule merging and aggregation process. The merging prompt guides LLMs to generalize conditions while preserving class separation; the aggregation prompt ensures self-consistency by retaining rule elements that are semantically stable across multiple merges.

the specific dataset. And **(2) Dual-Granularity Filtering**, which applies chunk-level suppression of dominant patterns and instance-level retention of rare samples, optimizing the synthetic distribution caused by the reuse of identical prompts.

#### A. Component I: Rule-Guided Generation

Unlike other modalities, tabular data often contain numerous irrelevant features and lack inherent structure, making it difficult for an LLM to capture feature-label relationships in limited reference data [29]. We address this with **Rule-Guided Generation**, which extracts these feature dependencies from limited tabular data  $D_{\text{train}}$  and insert them into the prompt. Importantly, these rules act as *soft guidance*: they guide the generation process toward reliable feature distribution without rigidly constraining the LLM's output. This guidance encourages generalization beyond rule-matched instances and prevents repetitive patterns commonly observed under general prompting. While using natural language to describe these *association rules* is convenient, they often lack structural precision and lead to semantic drift during generation [12]. We therefore represent rules as *if-then* statements extracted from the tree-based model, and apply an LLM-driven *merge-and-aggregation* procedure to unify and denoise the rule set. The complete workflow of Component I is summarized in Algorithm 1.

**1) Rules Extraction From Top-Performing Trees.** In prior work on tabular learning tasks, tree-based models have proven effective in capturing feature-label dependencies, largely due to their ability to fit the discrete and irregular structure of tabular data [30], [31]. Building on this observation, we extract association rules from decision trees, leveraging their inherent decision path to represent feature correlations. However, an individual decision tree is sensitive to noisy data, which can lead

---

#### Algorithm 1 Rule-Guided Generation

**Require:** Training dataset  $D_{\text{train}}$ , number of top trees  $k$ , number of runs  $G$

**Ensure:** Synthetic dataset  $D_{\text{syn}}$

```
1: RF  $\leftarrow$  TrainRandomForest( $D_{\text{train}}$ )
2: accList  $\leftarrow$  [Accuracy( $tree_i, D_{\text{train}}$ ) for each  $tree_i \in RF$ ]
3: RuleSet  $T \leftarrow$  SelectTopKTrees(RF, accList,  $k$ )
4: Initialize an empty list mergedSets
5: for  $i = 1$  to  $R$  do
6:   Initialize an empty list rawRules
7:   for each tree's rules  $\tau$  in  $T$  do
8:     rule  $r \leftarrow$  ExtractRule( $\tau, \ell$ )
9:     append  $r$  to rawRules
10:  end for
11:  merged  $R_i \leftarrow$  LLM_Merge(rawRules)
12:  append  $R_i$  to mergedSets
13: end for
14: Initialize an empty set  $\mathcal{R}$  and empty dataset  $D_{\text{syn}} \leftarrow \emptyset$ 
15: for each rule  $r$  in the union of all mergedSets do
16:   if count( $r, \text{mergedSets}$ )  $> G/2$  then
17:     add  $r$  to  $\mathcal{R}$ 
18:   end if
19: end for
20: for each rule  $r \in \mathcal{R}$  do
21:   prompt  $\pi \leftarrow$  ConstructPrompt( $r$ )
22:   samples  $\tilde{D} \leftarrow$  LLM_Generate( $\pi$ )
23:    $D_{\text{syn}} \leftarrow D_{\text{syn}} \cup \tilde{D}$ 
24: end for
25: return  $D_{\text{syn}}$ 
```

---

to unstable predictions [32]. Consequently, we instead adopt a small Random Forest (RF) to ensure robustness. Specifically, we train a RF on  $D_{\text{train}}$  and evaluate the predictive accuracy of each individual tree on the same data  $D_{\text{train}}$ , then ranked by their standalone accuracy and retain the top- $k$  (e.g.,  $k=3$ ) trees. These high-performance trees provide a compact and diverse set of decision paths (“*if-else*” rules) for subsequent rule extraction, ensuring coverage of key feature dependencies with minimal redundancy [33]–[35].

**2) Rules Merging and Aggregation.** Although decision rules from RF are individually interpretable, their overall structure across trees is redundant and inconsistent, making it difficult to directly consolidate them into coherent logic. This poses an issue: *how to unify a diverse set of “if-else” branches into a single rule that reflects feature-label dependencies*.

To address this, we design a two-step process that uses the LLM's reasoning capability to *merge* and *aggregate* symbolic *if-else* rules into a unified *if-then* format:

$$\text{If } [\text{Target}] = t, \text{ Then } C_1 \text{ and } C_2 \text{ and } \dots \text{ and } C_m \quad (1)$$

where  $t$  denotes a classification label, and each  $C_i$  is a predicate of the form  $x_j \circ v_j$ , with  $\circ \in \{<, \leq, >, \geq, =\}$ . This structure condenses complex tree-based decision paths into declarative rules that makes feature-label relationships explicit. Unlike the original “*if-else*” rules that predict labels

from features, the reformulated “*if-then*” format places the label in the premise, enabling the LLM to perform inverse reasoning and generate feature values consistent with the given target.

To obtain “*if-then*” rules, we apply the *Merge Logic prompt* (see Fig. 3), which takes the root-to-leaf rules from top- $k$  trees of the trained RF and aligns overlapping conditions for each class. It generalizes similar feature intervals while enforcing separation across classes, ensuring that each feature dimension for label  $t$  is represented by a single, non-overlapping interval. However, a single merge may retain spurious or inconsistent conditions due to conflicts and noise in the input paths from individual trees. To address this, we adopt a *self-consistency* strategy [36]: we perform  $G$  independent extraction + merge iterations and apply an *Aggregation Logic prompt* (see Fig. 3) to retain only stable rule elements. Conditions appearing in at least  $\lceil G/2 \rceil$  runs are kept, with their bounds averaged to form consensus intervals. This yields a association rules set  $\mathcal{R}$ , consisting of one robust conjunctive rule per label, as in (1).

This two-step LLM-guided process also *generalizes to regression*: By deriving output intervals from the tree-based model and applying the same rule unification procedure to generate one conjunctive rule per interval.

### 3) Tabular Data Generation via Rules-Guided Prompt.

To enhance the representation of semantically feature interactions, we generate tabular samples guided by the aggregated rules obtained in Component I. As illustrated in Fig. 2, each rule is transformed into a structured prompt that embeds its symbolic “*if-then*”, along with brief descriptions of all features to ensure semantic plausibility. These prompts are fed into an LLM to generate diverse and reliable consistent tabular samples, denoted as  $D_{\text{syn}}$ . The resulting  $D_{\text{syn}}$  subsequently serves as the input to Component II.

## B. Component II: Dual-Granularity Filtering

As shown in Fig. 2, synthetic data generated under low-data regimes often exhibit localized redundancy: over-representation of high-frequency modes and under-sampling of rare but informative modes. Prior methods typically employ instance-level filtering, but lack a global view of the overall distribution [16]. To address this challenge, we introduce **Dual-Granularity Filtering** as Component II, which aims to post-process the raw synthetic data  $D_{\text{syn}}$  by selectively filtering samples at two levels of granularity. The combined use of chunk-level and instance-level filters allows us to correct both global frequency distortion. *Chunk-level filtering* mitigates oversampling from the high-frequency subset, while *instance-level filtering* improves the quality of under-sampled instances from the low-frequency subset. The complete *Dual-Granularity Filtering* workflow is summarized in Algorithm 2, which takes the raw synthetic dataset  $D_{\text{syn}}$  as input and outputs a augmented synthetic dataset  $D_{\text{aug}}$  for downstream learning.

To make this filtering effective, we first estimate where and how redundancy occurs in  $D_{\text{syn}}$ . This is non-trivial in our low-data and mixed-type tabular setting, where LLM-generated samples lack explicit sampling probabilities [37]–[39].

---

### Algorithm 2 Dual-Granularity Filtering

---

**Require:** Training data  $\mathcal{D}_{\text{train}}$ , Synthetic data  $\mathcal{D}_{\text{syn}}$ , Candidate chunk sizes  $\mathcal{S}_{\text{cand}}$   
**Ensure:** Filtered augmented dataset  $\mathcal{D}_{\text{aug}}^*$

- 1: # Phase 1: Proxy-Based Redundancy Estimation
- 2: **for**  $x_i \in \mathcal{D}_{\text{syn}}$  **do**
- 3:   Find nearest seed  $s_j^* = \arg \min_{s_j \in \mathcal{D}_{\text{train}}} \text{DCR}(x_i, s_j)$
- 4: **end for**
- 5: Construct proxy distribution  $p = (p_1, \dots, p_n)$  and global redundancy ratio<sub>1</sub>  $\leftarrow G(p)$
- 6: # Phase 2: Frequency-Based Partitioning
- 7: Sort  $p$  to find permutation  $\pi$  where  $p_{\pi(1)} \geq \dots \geq p_{\pi(n)}$
- 8: Find smallest  $K$  such that  $\sum_{j=1}^K p_{\pi(j)} \geq \text{ratio}_1$
- 9: Partition  $\mathcal{D}_{\text{syn}}$  into  $\mathcal{D}_{\text{high}}$  (top- $K$  seeds) and  $\mathcal{D}_{\text{low}}$  (rest)
- 10: # Phase 3: Dual-Granularity Filtering
- 11: Initialize min\_surprisal  $\leftarrow \infty$ ,  $\mathcal{D}_{\text{aug}}^* \leftarrow \emptyset$
- 12: **for** each chunk size  $S \in \mathcal{S}_{\text{cand}}$  **do**
- 13:   # Chunk-level Filtering on  $\mathcal{D}_{\text{high}}$
- 14:   Partition  $\mathcal{D}_{\text{high}}$  into chunks  $\{\mathcal{C}_r\}$  of size  $S$
- 15:   Set ratio<sub>2</sub>  $\leftarrow A \ln(\text{ratio}_1) + B$
- 16:   Sort chunks by Score( $\mathcal{C}_r$ ) descending
- 17:    $\mathcal{D}_{\text{high\_filtered}} \leftarrow \text{union of top } \lfloor \text{ratio}_2 \cdot R \rfloor \text{ chunks}$
- 18:   # Instance-level Filtering on  $\mathcal{D}_{\text{low}}$
- 19:    $\mathcal{D}_{\text{low\_filtered}} \leftarrow \{x \in \mathcal{D}_{\text{low}} \mid \text{Conf}(x) \geq \text{Conf}_{\text{thresh}} \wedge \text{Uncert}(x) \leq \text{Uncert}_{\text{thresh}}\}$
- 20:   # Surprisal Evaluation
- 21:    $\mathcal{D}_{\text{aug}}(S) \leftarrow \mathcal{D}_{\text{high\_filtered}} \cup \mathcal{D}_{\text{low\_filtered}}$
- 22:   Train reference model  $M$  on  $\mathcal{D}_{\text{aug}}(S)$  and calculate Surprisal  $L(S)$  on  $\mathcal{D}_{\text{train}}$
- 23:   **if**  $L(S) < \text{min\_surprisal}$  **then**
- 24:     min\_surprisal  $\leftarrow L(S)$
- 25:      $\mathcal{D}_{\text{aug}}^* \leftarrow \mathcal{D}_{\text{aug}}(S)$
- 26:   **end if**
- 27: **end for**
- 28: **return**  $\mathcal{D}_{\text{aug}}^*$

---

### 1) Estimating Redundancy via Proxy-Based Frequency Analysis.

To support distribution-aware filtering, we introduce a *proxy-based* method to estimate local sampling frequencies with respect to the training set  $\mathcal{D}_{\text{train}}$ . We use the *Distance to Closest Record* (DCR) as a lightweight, task-agnostic heuristic to measure how each synthetic sample aligns with the training set [40], [41]. Specifically, for each synthetic sample  $x_i \in \mathcal{D}_{\text{syn}}$ , we assign it to its nearest training point  $s_j \in \mathcal{D}_{\text{train}}$  based on the DCR metric:

$$\text{Cluster}^*(i) = \arg \min_{1 \leq j \leq n} \text{DCR}(x_i, s_j). \quad (2)$$

By counting the number of synthetic data assigned to each seed and normalizing the result, we obtain a discrete *proxy distribution*  $p = (p_1, \dots, p_n)$ , where  $p_j$  reflects the local sampling frequency around seed  $s_j$ . To quantify localized

redundancy, we compute the *Gini coefficient*:

$$\text{ratio}_1 = G(p) = \frac{1}{n-1} \sum_{j=1}^n (2j - n - 1) p_{(j)}, \quad (3)$$

where  $p_{(1)} \leq \dots \leq p_{(n)}$  are the sorted components of the proxy distribution  $p$ . A larger  $G(p)$  indicates greater concentration of synthetic samples around fewer seeds, i.e., higher redundancy from  $\mathcal{D}_{\text{train}}$ .

Unlike entropy-based metrics, the Gini coefficient is more sensitive to sharp frequency disparities, especially in the presence of dominant high-frequency modes, while being less affected by sparse long-tail noise [42], [43]. This makes it well-suited for detecting localized redundancy in  $\mathcal{D}_{\text{syn}}$ . To enable generalization across settings, we use the global redundancy score  $\text{ratio}_1$  as a unified control signal, and further utilize  $\text{ratio}_1$  to partition the synthetic dataset by estimated sampling frequency. Specifically, we sort the training seeds in descending order of their proxy frequencies  $p_j$ , and identify the smallest index  $K$  such that  $\sum_{j=1}^K p_j \geq \text{ratio}_1$ . Synthetic samples associated with these top- $K$  seeds form the high-frequency subset  $\mathcal{D}_{\text{high}}$ , while the remaining samples constitute the low-frequency subset  $\mathcal{D}_{\text{low}} = \mathcal{D}_{\text{syn}} \setminus \mathcal{D}_{\text{high}}$ .

**2) Dual-Granularity Filtering.** Filtering synthetic samples is challenging due to the variability in localized redundancy and data quality across datasets [44], [45]. Given the partitioning into high-frequency ( $\mathcal{D}_{\text{high}}$ ) and low-frequency ( $\mathcal{D}_{\text{low}}$ ) subsets, we apply distinct filtering strategies at two levels of granularity. *Chunk-level filtering* targets redundancy in  $\mathcal{D}_{\text{high}}$ , while *instance-level filtering* focuses on improving quality within  $\mathcal{D}_{\text{low}}$ .

**2.1) Chunk-level Filtering in High-Frequency Subset.** High-frequency regions often contain subsets of highly similar samples, resulting from the generation pipeline. Evaluating individual samples in these regions is often noisy and ineffective, as over-sampled patterns tend to dominate locally. To address this, we apply a *chunk-level filtering* strategy that evaluates samples in groups based on their collective utility.

We randomly partition  $\mathcal{D}_{\text{high}}$  into non-overlapping chunks  $\{\mathcal{C}_1, \dots, \mathcal{C}_N\}$  of fixed size  $S$ . To assess the utility of each chunk, we train a lightweight reference model  $\mathcal{M}$  (e.g., XGBoost) on  $\mathcal{D}_{\text{train}}$ . For each synthetic pair  $(x, y)$ , we track the model  $\mathcal{M}$ 's prediction over  $T$  epochs and compute a correctness score indicating how frequently the model outputs the correct label with confidence:

$$\text{Correctness}(x, y) = \frac{1}{T} \sum_{t=1}^T \mathbf{1}(\mathbb{P}_{\mathcal{M}_t}(y | x) > 0.5), \quad (4)$$

where  $\mathcal{M}_t$  is the model at epoch  $t$ . The score of a chunk  $\mathcal{C}_r$  is then defined as the average correctness across its samples:

$$\text{Score}(\mathcal{C}_r) = \frac{1}{S} \sum_{(x_i, y_i) \in \mathcal{C}_r} \text{Correctness}(x_i, y_i). \quad (5)$$

Static thresholds often fail to generalize across datasets with different redundancy levels and can even exacerbate distributional bias. We introduce a log-scaled retention function that

adaptively determines the number of chunks to retain based on  $\text{ratio}_1$ :

$$\text{ratio}_2 = A \ln(\text{ratio}_1) + B, \quad (6)$$

where  $\text{ratio}_2 \in [0, 1]$  determines the retention rate. The logarithmic form ensures that retention is high when  $\text{ratio}_1$  is low, but flattens as  $\text{ratio}_1$  increases, encouraging stronger pruning under severe concentration. The coefficients  $A = 0.15$  and  $B = 0.55$  are empirically set, see Sec. V-F for details.

Finally, we sort all chunk scores in descending order and retain the top  $\lfloor \text{ratio}_2 \cdot N \rfloor$  chunks, enabling frequency-aware and efficient filtering within  $\mathcal{D}_{\text{high}}$ .

### 2.2) Instance-Level Filteringing in Low-Frequency Subset.

Samples in the low-frequency subset  $\mathcal{D}_{\text{low}}$  tend to reflect under-sampled regions of the feature space, which are more likely to contain useful variation but also noisy or unreliable outputs. To retain informative samples and discard potential outliers, we apply instance-level filtering guided by model confidence and predictive uncertainty.

For each sample  $(x, y) \in \mathcal{D}_{\text{low}}$ , we compute two quantities based on the reference model  $\mathcal{M}$ : the average confidence  $\text{Conf}(x)$  and the average predictive uncertainty  $\text{Uncert}(x)$ , both measured across training epochs. To make the filtering thresholds adaptive to data characteristics, we modulate them using  $\text{ratio}_1$ , such that higher redundancy yields looser acceptance criteria:

$$\begin{aligned} \text{Conf}_{\text{thresh}} &= \mu_{\text{conf}} - \text{ratio}_1 \cdot \sigma_{\text{conf}}, \\ \text{Uncert}_{\text{thresh}} &= \mu_{\text{uncert}} + \text{ratio}_1 \cdot \sigma_{\text{uncert}}, \end{aligned} \quad (7)$$

where  $\mu$  and  $\sigma$  denote the empirical mean and standard deviation over  $\mathcal{D}_{\text{low}}$ . A higher  $\text{ratio}_1$  yields more relaxed thresholds, allowing retention of uncertain but potentially informative samples; a lower  $\text{ratio}_1$  results in stricter filtering to suppress noise. A sample is retained if it satisfies both of the following conditions:

$$\text{Conf}(x) \geq \text{Conf}_{\text{thresh}} \quad \text{and} \quad \text{Uncert}(x) \leq \text{Uncert}_{\text{thresh}}.$$

By coupling  $\text{ratio}_1$  with two instance-level quantities, this mechanism effectively adapts filtering criteria across datasets with varying structural sparsity.

**2.3) Joint tuning via Surprisal.** The only remaining hyperparameter is the chunk size  $S$ , which determines the granularity of chunk-level evaluation in  $\mathcal{D}_{\text{high}}$ . However, synthetic datasets generated under different prompts or domains exhibit diverse frequency patterns, some contain tightly clustered modes while others are more diffuse. As a result, a fixed chunk size  $S$  may either over-segment homogeneous regions or obscure meaningful variation within diverse ones.

To balance stability and resolution, we adaptively select the optimal chunk size  $S$  using a *surprisal-based* criterion. For each candidate  $S$ , we apply *Dual-Granularity Filtering* to obtain an augmented dataset  $\mathcal{D}_{\text{aug}}(S)$ , on which the reference model  $\mathcal{M}$  via:

$$S^* = \arg \min_S \text{Surprisal}(\mathcal{D}_{\text{aug}}(S)) = -\frac{\sum_{i=1}^{|\mathcal{D}_{\text{train}}|} \log P_{\mathcal{M}}(y_i | x_i)}{|\mathcal{D}_{\text{train}}|}, \quad (8)$$

TABLE I  
**FEATURE NAMES AND HEADER TEST RESULTS.** **FEATURE NAMES TEST:** THE LLM INFERS COLUMN NAMES FROM SAMPLE ROWS. **HEADER TEST:** THE LLM COMPLETES THE HEADER AND FIRST FEW ROWS OF THE CSV. PERCENTAGES INDICATE ACCURACY FOR EACH DATASET AND LLM.

	GPT-4o-0806		GPT-3.5-turbo-1106		Qwen2.5-32b-Instruct		Qwen2.5-14b-Instruct	
	Feature Names	Header	Feature Names	Header	Feature Names	Header	Feature Names	Header
Other Datasets	0%	0%	0%	0%	0%	0%	0%	0%
Adult	86.67%	75.0%	86.67%	100.0%	0%*	25.0%	0%*	80.0%
Heart	100.0%	55.56%	25%	22.22%	0%	11.11%	0%	12.50%

\*Although no correct column names were produced, the LLM identified “*the Adult dataset from the UCI Machine Learning Repository*”

where  $P_{\mathcal{M}}(y_i \mid x_i)$  denotes the probability assigned to the true label by model  $\mathcal{M}$ . We search for the optimal chunk size  $S^*$  that minimizes the *surprisal* in (8), thereby encouraging filtered datasets that yield well-calibrated models aligned with the original data distribution. The final augmented dataset  $\mathcal{D}_{\text{aug}}^*$  is produced using this best-performing configuration.

While originally designed for classification, the *Dual-Granularity Filtering* framework readily generalizes to regression tasks. This is achieved by replacing classification-based scores with RMSE-based error measures, while retaining the overall structure of the pipeline with minimal changes.

## V. EXPERIMENT

In this section, we evaluate the effectiveness of the proposed **ReFine** framework on downstream machine learning tasks and conduct ablation studies to assess each design component. We begin by describing the experimental setup and baselines, followed by an analysis of the results.

### A. Datasets Selection

Many previous LLM-based tabular generation methods are evaluated on well-known public datasets (e.g., Adult, Heart, Housing) [15], [16], [21], [28], which may have been included in LLMs’ pretraining corpora [46]. This poses a risk of *data contamination*, where strong performance of these prompt-based LLM methods may result from memorization rather than true generalization, obscuring the real effectiveness of the generator based on the prompt method [47].

To mitigate this, we use an examination tool called **tab-memcheck** and select two of its tests [48]. The *Feature Names* checks whether the LLM can infer the correct column names without samples, while the *Header Test* evaluates whether the LLM can complete the CSV’s header and first data rows. We apply these tests to eight datasets, as summarized in Tab. II. Based on our results in Tab. I, only *adult* and *heart* are classified as **seen** datasets; the remaining six show no evidence of memorization and are classified as **unseen**.

### B. Baselines

We benchmark our method against two groups of baselines for tabular data generation and augmentation:

(1) *Non-LLM baselines*: including (i)CTGAN [9], a GAN-based model designed for tabular data generation; and (ii) TABSYN [11], a score-based generative model that achieves strong performance in sufficient-data settings.

TABLE II  
INFORMATION OF DATASETS USED

Dataset	Samples	Columns	Task	Creation Date
Disease	2149	35	Classification (2)	2024
Game	40034	12	Classification (3)	2024
Apple	4000	9	Classification (2)	2024
GPA	2392	15	Classification (5)	2024
Student	6607	22	Regression	2024
Farm	500	22	Regression	2025
Adult	32561	15	Classification (2)	2016
Heart	918	12	Classification (2)	2021

(2) *LLM-based baselines*: including (i) GREAT [15], which fine-tunes a pretrained GPT 2.5 for tabular data generation; (ii) EPIC [21], a prompting-based method that automates dataset construction through instruction-driven generation; and (iii) CLLM [16], which enhances LLM-generated data via curation.

### C. Experiment Setup

1) *Data Splits*: Following the problem formulation, we define the low-data regimes by setting the number of available training samples  $N \in \{30, 60, 90\}$ . For each dataset and each value of  $N$ , we construct the training set  $\mathcal{D}_{\text{train}}$  by independent and identically sampling  $N$  instances from the full real dataset  $\mathcal{D}_{\text{real}}$ . For classification datasets, we ensure that all target classes are equally represented in  $\mathcal{D}_{\text{train}}$ . The remaining samples are used as the test set  $\mathcal{D}_{\text{test}}$ . This sampling process is repeated 10 times with different random seeds to create multiple train-test splits. All generative models are evaluated using the same  $\mathcal{D}_{\text{train}}$  and  $\mathcal{D}_{\text{test}}$  across different values of  $N$  for fair comparison.

2) *Generation and Evaluation*: In Component I, our main experiments use GPT-3.5-Turbo-1106 for rules generation, GPT-3.5-Turbo-1106 for data generation [13]. Each baseline generates roughly 2,000 synthetic samples per dataset. In Component I, we fix  $k = 3$  for top- $k$  tree selection, and apply self-consistency to aggregate 5 independently sampled outputs. In Component II, we use XGBoost as the reference model  $\mathcal{M}$  for evaluating and tuning the filtering process [49]. We search over a range of candidate chunk sizes  $S \in \{20, 25, 30, \dots, 60\}$  when *joint tuning*.

To evaluate their downstream utility, we adopt the Machine Learning Efficiency (MLE) framework (*Train on Synthetic, Test on Real*) [9]–[11], [15], [16], [21]. Specifically, we sample

TABLE III

MAIN RESULTS ON BENCHMARK DATASETS. WE REPORT **F1 SCORE** FOR CLASSIFICATION TASKS AND **R<sup>2</sup>** FOR REGRESSION TASKS. UNSEEN DATASETS (I.E., NOT INCLUDED IN THE LLM’S MEMORY FOR LLM-BASED GENERATOR) ARE HIGHLIGHTED IN BLUE, AND SEEN DATASETS ARE HIGHLIGHTED IN RED. THE BEST RESULT IN EACH ROW IS SHOWN IN **BOLD**, AND THE SECOND-BEST RESULT IS UNDERLINED.

Original Data		Non-LLM Methods		LLM-Based Methods						
Datasets	Real Data	CTGAN	TABSYN	GREAT	EPIC	CLLM	I (w/o II)	II (w/o I)	I+II	
Disease (n=30)	93.68±1.4	44.58±4.7	54.79±2.7	46.54±1.7	32.01±8.2	61.89±2.1	59.61±1.5	62.07±1.7	<b>70.47±.83</b>	
Game (n=30)	86.0±.73	32.03±4.9	44.13±1.4	53.65±3.2	13.93±1.2	54.12±2.7	<u>56.44±2.2</u>	45.0±1.3	<b>59.24±2.8</b>	
Apple (n=30)	86.60±1.1	47.21±1.8	32.32±1.3	<u>59.91±2.3</u>	56.10±0.7	58.18±1.5	57.80±1.3	51.66±.12	<b>60.43±1.0</b>	
GPA (n=30)	47.29±.90	15.76±3.5	19.22±2.5	31.57±1.9	32.03±2.8	40.17±.46	<u>41.21±.97</u>	33.35±1.7	<b>44.06±.59</b>	
Student (n=30)	0.67±.07	-0.91±.12	0.14±.04	0.21±.03	0.35±.05	-0.11±.12	<u>0.37±.02</u>	0.08±.06	<b>0.38±.02</b>	
Farm (n=30)	-0.04±.03	-0.51±.06	-0.38±.05	-1.03±2.1	-0.68±.06	-0.29±.04	-0.44±.06	<b>-0.23±.06</b>	-0.30±.04	
Adult (n=30)	76.92±.68	50.47±4.1	62.83±3.2	67.45±1.3	61.94±3.3	<u>73.11±.65</u>	73.04±.59	72.77±.18	<b>74.90±.37</b>	
Heart (n=30)	86.71±1.7	48.16±8.8	79.40±1.3	80.74±1.3	81.20±1.3	80.47±.84	75.17±4.7	79.92±.24	<b>81.87±.33</b>	
Disease (n=60)	93.68±1.4	30.03±3.2	65.34±.93	52.80±3.1	44.05±7.8	66.86±1.1	75.65±2.5	62.81±2.2	<b>75.74±.77</b>	
Game (n=60)	86.0±.73	31.83±2.4	61.10±1.1	54.76±2.6	13.16±.0	<u>67.54±1.0</u>	61.39±2.6	59.81±1.1	<b>71.27±.42</b>	
Apple (n=60)	86.60±1.1	40.40±1.3	27.07±.68	60.33±1.6	<b>68.92±.85</b>	68.60±1.0	58.71±1.7	65.49±1.1	64.21±1.5	
GPA (n=60)	47.29±.90	18.11±3.3	28.48±1.8	35.60±2.4	32.19±3.5	33.17±1.1	44.34±.91	27.85±1.8	<b>48.42±.56</b>	
Student (n=60)	0.67±.07	-0.07±.05	-0.14±.14	0.02±.09	-0.63±.19	-0.48±.19	<u>0.27±.03</u>	-0.15±.04	<b>0.34±.07</b>	
Farm (n=60)	-0.04±.03	-0.22±.05	-0.17±.04	-0.16±.04	-0.21±.03	-0.30±.04	-0.21±.03	<b>-0.12±.02</b>	-0.15±.02	
Adult (n=60)	76.92±.68	47.55±5.1	63.58±1.6	69.70±.78	62.78±1.5	<b>73.94±.54</b>	73.28±.85	72.85±.50	73.48±.60	
Heart (n=60)	86.71±1.7	49.77±9.3	<u>81.35 ±1.2</u>	80.64±.82	77.55±1.6	80.33±.85	81.37±.96	79.13±.53	<b>81.98±.03</b>	
Disease (n=90)	93.68±1.4	47.18±3.5	69.90±2.0	65.32±1.4	30.03±3.2	<b>74.04±1.6</b>	69.74±1.5	66.54±1.2	<b>72.86±1.1</b>	
Game (n=90)	86.0±.73	33.67±2.5	<b>65.93±1.2</b>	61.17±3.0	13.16±.0	59.97±2.3	59.44±2.7	41.77±1.6	<b>63.87±2.7</b>	
Apple (n=90)	86.60±1.1	43.08±1.2	20.69±.61	64.23±2.6	<u>73.67±1.0</u>	73.43±.90	65.23±2.6	72.23±1.1	<b>75.04±1.5</b>	
GPA (n=90)	47.29±.90	14.91±2.3	34.51±1.3	36.19±1.1	16.28±1.98	41.79±1.1	<u>47.21±1.3</u>	38.98±.87	<b>49.21±.56</b>	
Student (n=90)	0.67±.07	-0.02±.01	-0.12±.10	0.22±.12	0.32±.07	-0.69±.13	<u>0.34±.09</u>	-0.27±.09	<b>0.47±.09</b>	
Farm (n=90)	-0.04±.03	-0.34±.03	<u>-0.15±.03</u>	-0.98±.71	-0.16±.04	-0.16±.02	-0.15±.03	<u>-0.14±.02</u>	<b>-0.13±.02</b>	
Adult (n=90)	76.92±.68	41.67±2.4	<u>69.77±.68</u>	71.52±.84	66.73±1.3	<u>74.11±.36</u>	<b>78.45±.97</b>	72.75±.51	72.87±.62	
Heart (n=90)	86.71±1.7	42.04±4.1	<u>81.43 ±1.3</u>	81.05±.88	77.65±1.7	81.23±1.0	<b>82.44±.86</b>	78.40±1.4	80.08±.03	
Avg Rank	-	<b>7.2</b>	<b>5.1</b>	<b>4.8</b>	<b>5.8</b>	<b>3.7</b>	<b>3.2</b>	<b>4.5</b>	<b>1.6</b>	

1,000 synthetic points under 10 different random seeds to train an XGBoost model, and evaluate it on the original real dataset. Final results are reported as the average performance across all seeds. For *Evaluation Metric*, we use standard downstream metrics for evaluation: **F1 score** for classification tasks and **R<sup>2</sup>** (coefficient of determination) for regression tasks.

#### D. Main Results

Tab. III reports the downstream performance of **ReFine** and representative baselines under three low-data regimes ( $N \in \{30, 60, 90\}$ ). **ReFine** attains the best score on every task, with an average rank of **1.6**. On **unseen datasets** it improves  $R^2$  by as much as **0.44** and  $F_1$  by up to **10.0%** relative to the strongest prior method (CLLM), evidencing robust generalization. The full **ReFine** framework (I+II) outperforms its individual components, achieving higher average ranks across benchmarks. This suggests the integration of both components contributes positively to overall effectiveness.

LLM-based approaches overall outperform non-LLM models in low-data settings, likely due to their stronger capacity for structured generation and contextual generalization. However, performance varies significantly among LLM-based methods. EPIC and GREAT lack explicit generation guidance, which limits their ability to enforce meaningful structure in synthetic data. **ReFine** addresses this by embedding association rules

into the generation process, improving both accuracy and consistency. CLLM incorporates instance-level filtering but cannot correct redundancy in the synthetic data. By incorporating association rules during generation, **ReFine** yields more accurate and consistent data, with the largest margins on regression benchmarks.

Some LLM-based methods perform well on **seen datasets** but degrade notably on **unseen datasets**. This discrepancy aligns with the *data contamination risk* highlighted in our datasets selection—performance gains may in part reflect memorization from pretraining rather than true generalization. In contrast, **ReFine** maintains stable performance across both, validating its capability for genuine generalization in practical scenarios.

#### E. Ablation Study in Component I

To systematically assess the contribution of each submodule in **Component I**, we design two sets of experiments that address the following questions: (1) Q1: Does Rule Design Enhance Generation Quality? (2) Q2: Can Rule-Based Methods Generalize Across LLMs? and conclude with a qualitative (3) case study illustrating representative rules in action. Throughout this section we fix  $N = 30$  and conduct on *Disease* (binary classification), *GPA* (multi-classification), and *Student* (regression).

TABLE IV

MAIN RESULTS ON BENCHMARK DATASETS ( $n=30$ ). WE REPORT **F1 SCORE** FOR CLASSIFICATION TASKS AND **R<sup>2</sup>** FOR REGRESSION TASKS. THE BEST RESULT IN EACH ROW IS SHOWN IN **BOLD**.

Original Data		Rules Generator	Data Generator		
Datasets	Real Data		Qwen2.5-14b-Instruct	Qwen2.5-32b-Instruct	GPT-4o-0806
Disease	93.68 $\pm$ 1.4	No Rules	59.52 $\pm$ 1.9	65.12 $\pm$ 2.3	62.26 $\pm$ 3.2
		Qwen2.5-32b-Instruct	66.34 $\pm$ 1.4	70.16 $\pm$ .80	67.38 $\pm$ .85
		GPT-4o-0806	<b>70.21 <math>\pm</math> 1.9</b>	67.74 $\pm$ 1.4	64.04 $\pm$ 2.7
GPA	47.29 $\pm$ .90	No Rules	20.67 $\pm$ .87	30.23 $\pm$ 1.4	27.58 $\pm$ 2.3
		Qwen2.5-32b-Instruct	40.62 $\pm$ 1.4	39.13 $\pm$ 3.4	<b>47.07 <math>\pm</math> .5</b>
		GPT-4o-0806	42.25 $\pm$ 1.4	31.99 $\pm$ 2.9	44.34 $\pm$ 0.6
Student	0.67 $\pm$ .07	No Rules	0.25 $\pm$ .04	0.32 $\pm$ .03	-1.29 $\pm$ .27
		Qwen2.5-32b-Instruct	0.30 $\pm$ .03	<b>0.33 <math>\pm</math> .03</b>	0.25 $\pm$ .01
		GPT-4o-0806	0.18 $\pm$ .05	-0.38 $\pm$ .16	-0.01 $\pm$ .14

#### “If-Then” Rule Form

- If Diagnosis = 1:
  - Then MMSE  $\leq$  16.85 and FunctionalAssessment < 6.90
- If Diagnosis = 0:
  - Then MMSE > 18.85 and FunctionalAssessment > 6.90

#### Natural Language Rule Form

- There is a noticeable trend where patients diagnosed with Alzheimer’s often have lower MMSE scores. This trend is particularly apparent among older patients, suggesting a strong association between advanced age, decreased cognitive function, and an Alzheimer’s diagnosis. The lower functional assessment scores in these individuals further support this link, indicating that cognitive decline is a key factor in distinguishing those with Alzheimer’s.

Fig. 4. Illustrative “if-then” Form and its Natural-Language paraphrase derived from the *Disease* dataset ( $N=30$ ).

#### Q1: Does Rule Design Enhance Generation Quality?

To investigate the impact of rule design on generation quality, we decompose this question into two sub-components: 1) the effect of *rule format*, and 2) the effect of *rule aggregation strategy*. In all experiments, we fix the backbone settings (GPT-4o-0806 as Rule Generator and GPT-3.5-turbo-1106 as Data Generator) and evaluate results via MLE score.

##### 1) Rule Format Comparison.

To gauge whether the *explicit* “if-then” representation is essential to the success of Rule-Guided Generation, we recast every Random-Forest path into two formats: (i) its original “If-

TABLE VI

PERFORMANCE UNDER DIFFERENT AGGREGATION STRATEGIES. WE REPORT **F1 SCORE** FOR DISEASE AND GPA, AND **R<sup>2</sup>** FOR STUDENT.

	Single-Pass	COT	Self-Consistency
Disease	54.26 $\pm$ 3.2	58.46 $\pm$ .98	<b>59.61 <math>\pm</math> 1.5</b>
GPA	24.80 $\pm$ 4.0	38.48 $\pm$ .82	<b>41.21 <math>\pm</math> .97</b>
Student	0.35 $\pm$ .06	0.35 $\pm$ .02	<b>0.37 <math>\pm</math> .02</b>

Then” clause and (ii) a concise natural-language paraphrase, which automatically produced by prompting the LLM to restate each path in natural language. These two formats reflect two distinct rule-extraction schemes. A side-by-side example of the two rule forms is shown in Fig. 4.

As shown in Tab. V, *if-then* rules outperform both natural-language rules and the No-Rule baseline, demonstrating the benefit of symbolic structure. While both rule-based approaches surpass the baseline, the symbolic form delivers more reliable performance. This advantage stems from two key factors: (i) Random Forests extract concise and faithful feature-label dependencies even in low-data settings, and (ii) the *If-Then* format retains explicit numeric boundaries and dependent constraints, unlike natural language, which tends to weaken precision [50]. By guiding generation through explicit symbolic rules, the LLM is directed toward semantically coherent subspaces, resulting in higher-quality samples.

##### 2) Robustness of Rule Aggregation Strategy.

Next, we evaluate how different rule aggregation strategies affect data quality. We compare our proposed **Self-Consistency aggregation** (described in Sec. IV-A) against two alternatives: (i) **Single-Pass**, which merges rules in one step without verification, and (ii) **Chain-of-Thought (CoT)** prompting, which guides the LLM to reason step-by-step during rule consolidation [51].

Results in Tab. VI reveal that both **Single-Pass** and **CoT** aggregation yield less consistent performance across datasets. Their reliance on one-shot reasoning makes them vulnerable to local inconsistencies and stochastic behavior in LLM outputs. In contrast, self-consistency aggregation enforces cross-run

TABLE V

PERFORMANCE UNDER DIFFERENT RULE REPRESENTATIONS. WE REPORT **F1 SCORE** FOR DISEASE AND GPA, AND **R<sup>2</sup>** FOR STUDENT.

	No Rule	Natural Language	“if-then” Form
Disease	49.13 $\pm$ 1.2	57.54 $\pm$ 1.7	<b>59.61 <math>\pm</math> 1.5</b>
GPA	24.80 $\pm$ 4.0	37.78 $\pm$ .60	<b>41.21 <math>\pm</math> .97</b>
Student	-0.11 $\pm$ .12	-0.79 $\pm$ .53	<b>0.37 <math>\pm</math> .02</b>

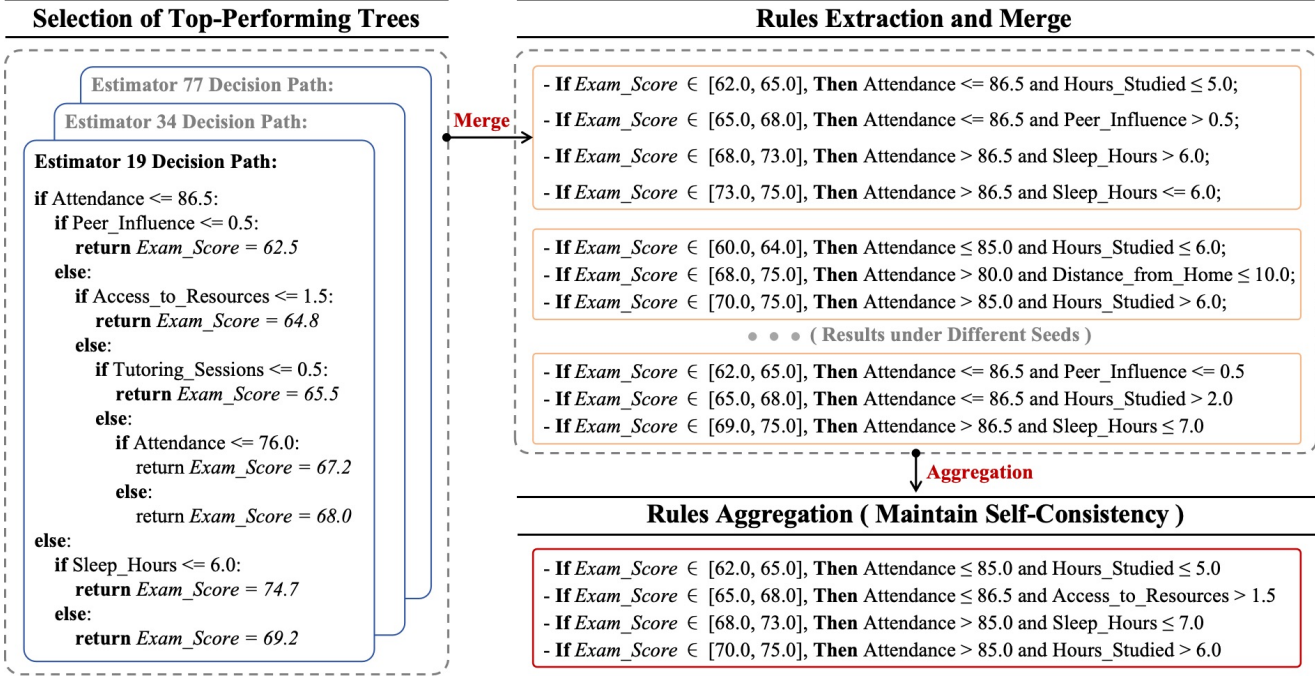


Fig. 5. Case study for Component I on the *Student* dataset. Noisy tree paths are distilled into a self-consistent symbolic rule set that refines the underlying feature dependencies and later guides downstream data generation. A detailed analysis is provided in Sec. V-E.

agreement and filters out unstable logic fragments, leading to more robust rule sets and better downstream fidelity.

### 3) Conclusion.

Together, these experiments confirm that both the **structure of association rules** and the **robustness of their consolidation** play a vital role in synthetic data quality. Structured, verified logic provides a strong inductive prior that is especially valuable in low-data regimes, where models benefit from symbolic scaffolding to recover sparse but critical relationships.

### Q2: Can Rule-Based Methods Generalize Across LLMs?

To evaluate the robustness of *Rule-Guided Generation* in different LLM backbones, we compare performance using the MLE under varying combinations of rules generators and data generators. The result as shown in Tab. IV, across all tested LLMs which ranging from mid-sized (Qwen2.5-14b) to larger models (Qwen2.5-32b and GPT-4o), the introduction of association rules consistently improves the quality of synthetic data. Notably, even when rules are extracted by weaker models (e.g., Qwen2.5-32b), stronger models like GPT-4o still benefit from them—highlighting that rule-based guidance contributes independently of LLMs capacity. This demonstrates the generality and transferability of our design.

### Illustrative Example of Rule Merging & Aggregation.

To illustrate the practical functioning of **Component I**, we present a case study demonstrating how symbolic rules are distilled into interpretable *if-then* forms through rule merging and aggregation. Intermediate outcomes are visualized in Fig. 5. In this example, decision trees from the trained random forest exhibit conflicting paths—for example, assigning different *Exam\_Score* values to overlapping input regions such as

$Attendance \leq 86.5$  and  $Attendance \leq 76.0$ . The merging phase addresses these inconsistencies by consolidating noisy rule fragments into coherent patterns, such as those involving *Sleep\_Hours*. To improve robustness, the training and merging process is repeated under multiple random seeds. The aggregation step then retains only those patterns that appear consistently across runs, thereby filtering out unstable conditions and enforcing self-consistency.

This case highlights two key strengths of Component I: (1) it distills noisy and fragmented tree logic into compact rules that capture meaningful relationships in low-data regimes; (2) it produces one concise association rule per segment, enhancing both interpretability and generation quality.

### F. Ablation Study in Component II

To systematically examine the design choices within **Component II**, we design two sets of experiments that address the following questions: (1) Q3: How Effective Are Instance-Level and Chunk-Level Filters Individually? (2) Q4: How Reliable Is the Gini Coefficient as an Redundancy Metric? and conclude with a (3) case study illustrating representative rules.

Throughout this section, we still report results on *Disease* (binary classification), *GPA* (multi-class classification), and *Student* (regression). All experiments in this section use the same rule/data generation backbone (GPT-4o-0806 and GPT-3.5-turbo-1106, respectively).

### Q3: How Effective Are Instance-Level and Chunk-Level Filters Individually?

To assess the impact of filtering granularity within **Component II**, we compare three strategies for data selection: (i)

TABLE VII

PERFORMANCE UNDER DIFFERENT AGGREGATION STRATEGIES. WE REPORT **F1 SCORE** FOR DISEASE AND GPA, AND **R<sup>2</sup>** FOR STUDENT.

	Instance-Level Only	Chunk-Level Only	Dual-Granularity
Disease (n=30)	69.29 $\pm$ .38	63.88 $\pm$ .94	<b>70.47 <math>\pm</math> .83</b>
GPA (n=30)	39.39 $\pm$ 1.0	41.02 $\pm$ .81	<b>44.06 <math>\pm</math> .59</b>
Student (n=30)	<b>0.39 <math>\pm</math> .01</b>	0.35 $\pm$ .01	0.38 $\pm$ .02
Disease (n=60)	73.13 $\pm$ 1.11	68.81 $\pm$ 1.6	<b>75.74 <math>\pm</math> .77</b>
GPA (n=60)	43.25 $\pm$ .0	45.04 $\pm$ .54	<b>48.42 <math>\pm</math> .56</b>
Student (n=60)	0.32 $\pm$ .02	0.19 $\pm$ .02	<b>0.34 <math>\pm</math> .07</b>
Disease (n=90)	71.65 $\pm$ .89	71.97 $\pm$ 1.2	<b>72.86 <math>\pm</math> 1.1</b>
GPA (n=90)	47.62 $\pm$ .41	46.55 $\pm$ .80	<b>49.21 <math>\pm</math> .56</b>
Student (n=90)	0.45 $\pm$ .02	0.38 $\pm$ .02	<b>0.47 <math>\pm</math> .09</b>

**instance-level only**, which evaluates each instance independently; (ii) **chunk-level only**, which scores and filters batches of samples as a chunk; and (iii) a combined **dual-granularity** strategy that integrates signals from both levels.

As shown in Tab. VII, the dual-granularity approach consistently achieves the best downstream performance across all datasets and data regimes, outperforming either instance-level or chunk-level filtering alone. The consistent gains illustrate that the two strategies are complementary: instance-level scores help identify and remove low-quality individual samples, while chunk-level scores capture broader distributional trends. By fusing both signals, the filter suppresses the repetitive, high-frequency patterns favored by LLMs. This dual-granularity perspective directly mitigates the localized redundancy introduced by batch generation, yielding synthetic data that is simultaneously cleaner and more diverse, and thereby boosting downstream performance.

#### Q4: How Reliable Is the Gini Coefficient as an Redundancy Metric?

To assess the robustness and suitability of the *Gini coefficient* defined in (3) as an redundancy control metric in Component II, we conduct three evaluations: 1) stability across sample sizes, 2) impact on the log-scaled retention function, and 3) effectiveness relative to alternative metrics.

##### 1) Stability Under Varying Generation Sizes

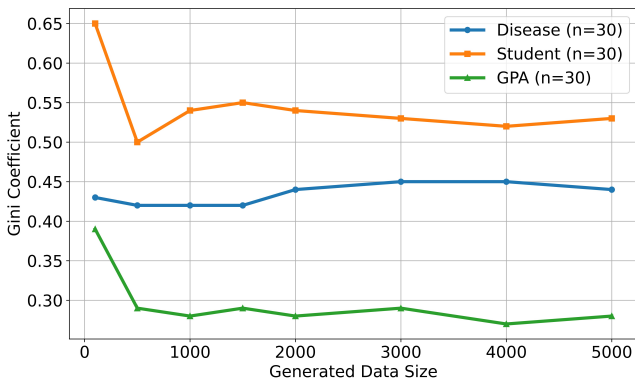


Fig. 6. Gini coefficient under different synthetic data sizes.

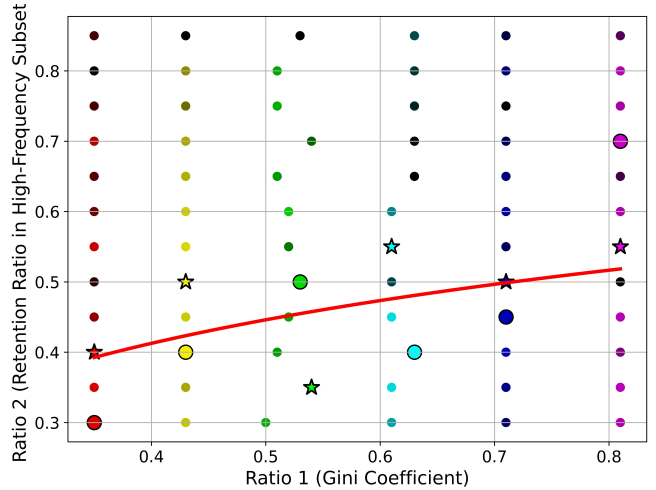


Fig. 7. Scatter plot of *Ratio 1* (Gini coefficient) versus *Ratio 2* (retention in high-frequency subset). Point color indicates downstream model performance after filtering, with lighter colors representing higher performance and darker colors indicating lower performance. In each group, the star (\*) marks the best-performing point and the circle (o) marks the second-best.

We assess the Gini coefficient’s sensitivity to sample size of synthetic data, as the control signal should be scale-invariant; any dependence on generation count would propagate instability throughout the filtering pipeline.

As shown in Fig. 6, the Gini coefficient quickly stabilizes after approximately 1,000 samples across all evaluated tasks, with minimal fluctuation thereafter. This indicates that the major distributional modes are formed early in the generation process and that Gini offers a consistent, scale-invariant signal for downstream filtering decisions.

##### 2) Impact on the Log-Scaled Retention Function.

Using the log-scaled mapping in (6), we vary  $\text{ratio}_1 = G(p)$  across its empirical range and record the resulting  $\text{ratio}_2$  as well as downstream F1. Fig. 7 shows that performance peaks at intermediate retention, validating that the Gini-driven schedule prunes aggressively only when redundancy is severe, while preserving diversity in more balanced settings. We observe that the Gini values across datasets tend to lie in a relatively narrow and stable range, which contributes to the robustness of

TABLE VIII  
COMPARISON OF GINI AND ENTROPY FILTERING.

	Gini		Entropy	
	Value	MLE	Value	MLE
Disease (n=30)	0.40	<b>70.47 <math>\pm</math> .83</b>	0.13	68.87 $\pm$ .57
GPA (n=30)	0.23	<b>44.06 <math>\pm</math> .59</b>	0.06	39.88 $\pm$ .83
Student (n=30)	0.58	<b>0.38 <math>\pm</math> .02</b>	0.31	0.36 $\pm$ .01
Disease (n=60)	0.68	<b>75.74 <math>\pm</math> .77</b>	0.30	72.03 $\pm$ .33
GPA (n=60)	0.23	<b>48.42 <math>\pm</math> .56</b>	0.03	38.53 $\pm$ .83
Student (n=60)	0.61	<b>0.34 <math>\pm</math> .07</b>	0.20	0.31 $\pm$ .04
Disease (n=90)	0.40	72.86 $\pm$ 1.1	0.21	<b>73.97 <math>\pm</math> 1.5</b>
GPA (n=90)	0.25	<b>49.21 <math>\pm</math> .56</b>	0.02	46.91 $\pm$ .76
Student (n=90)	0.58	<b>0.47 <math>\pm</math> .09</b>	0.20	0.43 $\pm$ .05

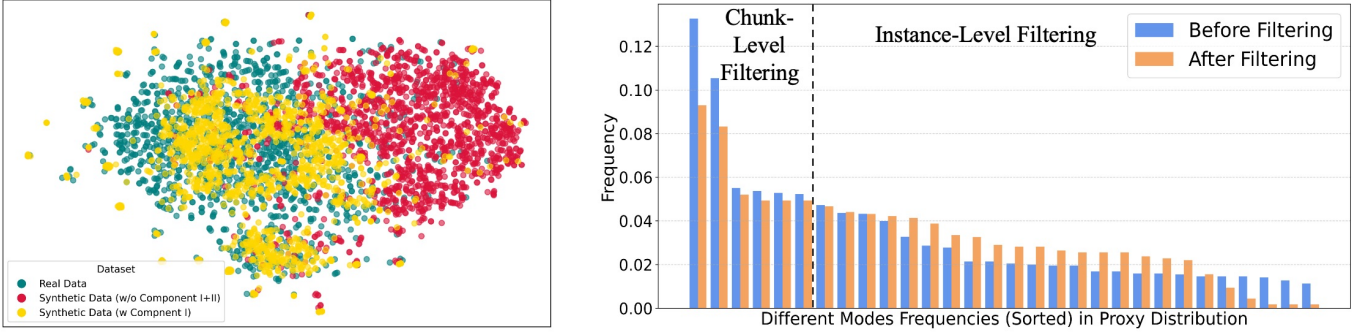


Fig. 8. (Left) t-SNE plot showing that *Rule-Guided Generation* (yellow, w/ Component I) aligns more closely with *Real Data* (green) than generation without rule guidance (red). (Right) Proxy mode frequencies before (blue) and after (orange) *dual-granularity filtering* (Component II), where filtering reduces over-sampled high-frequency modes and improves coverage of low-frequency regions.

the fitted retention schedule. As a result, the coefficients  $A = 0.15$  and  $B = 0.55$ , derived from cross-dataset regression, generalize well without tuning.

### 3) Comparison Against Entropy-Based Filtering

We then assess whether Gini is not only stable, but also *effective* at guiding filtering. To this end, we substitute Gini with entropy—another distribution metric—in our dual-granularity pipeline and compare the resulting MLE scores.

As shown in Table VIII, Gini-guided filtering consistently outperforms the entropy variant across datasets and data regimes. This superiority is especially pronounced in low-data regimes, where redundancy has the greatest impact on model generalization. Gini and entropy differ fundamentally in how they respond to localized redundancy [43]. Gini emphasizes inequality among the high-frequency subset, making it more responsive to dominant sampling modes. Entropy, by contrast, distributes sensitivity across all regions, including a low-frequency subset, which may contain noise or irrelevant variation [42], [52]. This causes entropy to underestimate concentration and weaken filtering in the high-frequency subset.

This distinction is crucial for tabular data generation, where synthetic samples often cluster around prompt-aligned guides. Filtering must respond to overrepresented regions without overreacting to noise. Gini's inductive steer aligns naturally with this requirement, making it a more effective control signal than entropy in our setting.

### G. Component-wise Distributional Analysis

This section examines the distributional impact of Component I and Component II on the generated synthetic data. As shown in the left panel of Fig. 8, synthetic data generated with *rule-guided guidance* (yellow) exhibits greater alignment with real data (green) compared to the baseline model without *rule-guided guidance* (red), as reflected in their overlapping t-SNE distributions. This indicates that Component I helps align the global structure of synthetic data by guiding it to an interpretable feature–label dependencies. However, dense clustering in certain regions remains apparent, indicating residual mode redundancy.

The right panel of Fig. 8 illustrates the impact of Component II by comparing sorted mode frequencies in the proxy distribution, before and after applying the *dual-granularity filtering* mechanism. The high-frequency subset (left bars) is significantly suppressed after filtering, while the low-frequency subset (right bars) is more equally represented. This confirms that Component II effectively flattens distributional spikes and improves sample coverage across the feature space. These results demonstrate the distinct yet synergistic roles of the two components: Component I enhances alignment with the underlying feature distribution of real data, while Component II addresses localized redundancy by promoting balanced mode coverage.

## VI. CONCLUSION

We present **ReFine**, a two-component framework that addresses fundamental limitations of prompt-based LLM tabular generation in low-data regimes. Our approach integrates symbolic *if-then* rules derived from interpretable models to enforce domain-specific feature distribution, while employing dual-granularity filtering to mitigate localized redundancy inherent in batch generation processes. The framework demonstrates consistent improvements across diverse benchmarks, achieving up to 0.44 absolute gain in  $R^2$  and 10% relative improvement in  $F_1$  over existing methods. Component-wise analysis reveals that rule-guided generation effectively captures dataset-specific dependencies often overlooked by pre-trained models, while dual-granularity filtering successfully rebalances synthetic distributions through coordinated chunk-level and instance-level selection strategies. Nevertheless, the current implementation of chunk-level retention utilizes empirically derived logarithmic scaling, potentially limiting generalizability under extreme distributional scenarios. Future research directions include exploring adaptive retention functions and establishing theoretical foundations for improved cross-domain robustness and generalization. We leave this as an avenue for future work.

## REFERENCES

[1] O. Benjelloun, S. Chen, and N. Noy, “Google dataset search by the numbers,” in *International semantic web conference*. Springer, 2020, pp. 667–682.

[2] S. P. Ghosh, “Statistical relational tables for statistical database management,” *IEEE Transactions on Software Engineering*, no. 12, pp. 1106–1116, 2012.

[3] X. Yang, M. Zhang, J. Fan, Z. Luo, and Y. Yang, “A multi-task learning framework for reading comprehension of scientific tabular data,” in *2024 IEEE 40th International Conference on Data Engineering (ICDE)*. IEEE, 2024, pp. 3710–3724.

[4] A. Shankar, H. Brouwer, R. Hai, and L. Chen, “S i l o f use: Cross-silo synthetic data generation with latent tabular diffusion models,” in *2024 IEEE 40th International Conference on Data Engineering (ICDE)*. IEEE, 2024, pp. 110–123.

[5] A. X. Wang, S. S. Chukova, C. R. Simpson, and B. P. Nguyen, “Challenges and opportunities of generative models on tabular data,” *Applied Soft Computing*, p. 112223, 2024.

[6] B. Kovalerchuk and E. Vityaev, *Data mining in finance: advances in relational and hybrid methods*. Springer Science & Business Media, 2005, vol. 547.

[7] Z. Ji, Z. C. Lipton, and C. Elkan, “Differential privacy and machine learning: a survey and review,” *arXiv preprint arXiv:1412.7584*, 2014.

[8] M. Hernandez, G. Epelde, A. Alberdi, R. Cilla, and D. Rankin, “Synthetic data generation for tabular health records: A systematic review,” *Neurocomputing*, vol. 493, pp. 28–45, 2022.

[9] L. Xu, M. Skoularidou, A. Cuesta-Infante, and K. Veeramachaneni, “Modeling tabular data using conditional gan,” *Advances in neural information processing systems*, vol. 32, 2019.

[10] A. Kotelnikov, D. Baranchuk, I. Rubachev, and A. Babenko, “Tabddpm: Modelling tabular data with diffusion models,” in *International Conference on Machine Learning*. PMLR, 2023, pp. 17564–17579.

[11] H. Zhang, J. Zhang, B. Srinivasan, Z. Shen, X. Qin, C. Faloutsos, H. Rangwala, and G. Karypis, “Mixed-type tabular data synthesis with score-based diffusion in latent space,” in *The twelfth International Conference on Learning Representations*, 2024.

[12] X. Fang, W. Xu, F. A. Tan, J. Zhang, Z. Hu, Y. Qi, S. Nickleach, D. Socolinsky, S. Sengamedu, and C. Faloutsos, “Large language models (llms) on tabular data: Prediction, generation, and understanding—a survey,” *arXiv preprint arXiv:2402.17944*, 2024.

[13] T. Brown, B. Mann, N. Ryder, M. Subbiah, J. D. Kaplan, P. Dhariwal, A. Neelakantan, P. Shyam, G. Sastry, A. Askell *et al.*, “Language models are few-shot learners,” *Advances in neural information processing systems*, vol. 33, pp. 1877–1901, 2020.

[14] T. Kojima, S. S. Gu, M. Reid, Y. Matsuo, and Y. Iwasawa, “Large language models are zero-shot reasoners,” *Advances in neural information processing systems*, vol. 35, pp. 22199–22213, 2022.

[15] V. Borisov, K. Seßler, T. Leemann, M. Pawelczyk, and G. Kasneci, “Language models are realistic tabular data generators,” in *ICLR*, 2023.

[16] N. Seedat, N. Huynh, B. Van Breugel, and M. Van Der Schaar, “Curated llm: Synergy of llms and data curation for tabular augmentation in low-data regimes,” *arXiv preprint arXiv:2312.12112*, 2023.

[17] P. Raghavan and N. El Gayar, “Fraud detection using machine learning and deep learning,” in *2019 international conference on computational intelligence and knowledge economy (ICCIKE)*. IEEE, 2019, pp. 334–339.

[18] Z. Li, X. Li, Z. Duan, B. Dong, N. Liu, and J. Wang, “Toward a unified framework for unsupervised complex tabular reasoning,” in *2023 IEEE 39th International Conference on Data Engineering (ICDE)*. IEEE, 2023, pp. 1691–1704.

[19] S. Bommareddy, J. A. Khan, R. Anand *et al.*, “A review on healthcare data privacy and security,” *Networking Technologies in Smart Healthcare*, pp. 165–187, 2022.

[20] B. Zhang, C. Luo, D. Yu, X. Li, H. Lin, Y. Ye, and B. Zhang, “Metadiff: Meta-learning with conditional diffusion for few-shot learning,” in *Proceedings of the AAAI conference on artificial intelligence*, vol. 38, no. 15, 2024, pp. 16687–16695.

[21] J. Kim, T. Kim, and J. Choo, “Epic: Effective prompting for imbalanced-class data synthesis in tabular data classification via large language models,” *Advances in Neural Information Processing Systems*, vol. 37, pp. 31504–31542, 2024.

[22] T. Zhong, Z. Yang, Z. Liu, R. Zhang, Y. Liu, H. Sun, Y. Pan, Y. Li, Y. Zhou, H. Jiang *et al.*, “Opportunities and challenges of large language models for low-resource languages in humanities research,” *arXiv preprint arXiv:2412.04497*, 2024.

[23] P. Sahoo, A. K. Singh, S. Saha, V. Jain, S. Mondal, and A. Chadha, “A systematic survey of prompt engineering in large language models: Techniques and applications,” *arXiv preprint arXiv:2402.07927*, 2024.

[24] M. C. Stoian, S. Dyrmschi, M. Cordy, T. Lukasiewicz, and E. Giunchiglia, “How realistic is your synthetic data? constraining deep generative models for tabular data,” in *The Twelfth International Conference on Learning Representations*, 2024.

[25] X. Amatriain, “Prompt design and engineering: Introduction and advanced methods,” *arXiv preprint arXiv:2401.14423*, 2024.

[26] P. Liu, W. Yuan, J. Fu, Z. Jiang, H. Hayashi, and G. Neubig, “Pre-train, prompt, and predict: A systematic survey of prompting methods in natural language processing,” *ACM computing surveys*, vol. 55, no. 9, pp. 1–35, 2023.

[27] R. Zevallos, M. Farrús, and N. Bel, “Frequency balanced datasets lead to better language models,” in *Findings of the Association for Computational Linguistics: EMNLP 2023*, 2023, pp. 7859–7872.

[28] Y. Wang, D. Feng, Y. Dai, Z. Chen, J. Huang, S. Ananiadou, Q. Xie, and H. Wang, “Harmonic: Harnessing llms for tabular data synthesis and privacy protection,” in *The Thirty-eighth Conference on Neural Information Processing Systems Datasets and Benchmarks Track*, 2024.

[29] X. Fang, W. Xu, F. A. Tan, J. Zhang, Z. Hu, Y. J. Qi, S. Nickleach, D. Socolinsky, S. Srinivasan Sengamedu, and C. Faloutsos, “Large language models (llms) on tabular data: Prediction, generation, and understanding - a survey,” *Transactions on Machine Learning Research*, 2024.

[30] L. Grinsztajn, E. Oyallon, and G. Varoquaux, “Why do tree-based models still outperform deep learning on typical tabular data?” *Advances in neural information processing systems*, vol. 35, pp. 507–520, 2022.

[31] R. Shwartz-Ziv and A. Armon, “Tabular data: Deep learning is not all you need,” *Information Fusion*, vol. 81, pp. 84–90, 2022.

[32] Y. Wu, K.-H. Chow, W. Wei, and L. Liu, “Hierarchical pruning of deep ensembles with focal diversity,” *ACM Transactions on Intelligent Systems and Technology*, vol. 15, no. 1, pp. 1–24, 2024.

[33] V. Y. Kulkarni and P. K. Sinha, “Pruning of random forest classifiers: A survey and future directions,” in *2012 International Conference on Data Science & Engineering (ICDSE)*. IEEE, 2012, pp. 64–68.

[34] M. Azad, T. H. Nehal, and M. Moshkov, “A novel ensemble learning method using majority based voting of multiple selective decision trees,” *Computing*, vol. 107, no. 1, p. 42, 2025.

[35] A. A. Khan, O. Chaudhari, and R. Chandra, “A review of ensemble learning and data augmentation models for class imbalanced problems: Combination, implementation and evaluation,” *Expert Systems with Applications*, vol. 244, p. 122778, 2024.

[36] X. Wang, J. Wei, D. Schuurmans, Q. V. Le, E. H. Chi, S. Narang, A. Chowdhery, and D. Zhou, “Self-consistency improves chain of thought reasoning in language models,” in *The Eleventh International Conference on Learning Representations*, 2023.

[37] V. Sehwag, S. Mahloujifar, T. Handina, S. Dai, C. Xiang, M. Chiang, and P. Mittal, “Robust learning meets generative models: Can proxy distributions improve adversarial robustness?” in *International Conference on Learning Representations*, 2021.

[38] ———, “Improving adversarial robustness using proxy distributions,” *arXiv preprint arXiv:2104.09425*, vol. 1, 2021.

[39] J. Wu, S. Yang, R. Zhan, Y. Yuan, L. S. Chao, and D. F. Wong, “A survey on llm-generated text detection: Necessity, methods, and future directions,” *Computational Linguistics*, pp. 1–66, 2025.

[40] P. A. Osorio-Marulanda, G. Epelde, M. Hernandez, I. Isasa, N. M. Reyes, and A. B. Iraola, “Privacy mechanisms and evaluation metrics for synthetic data generation: A systematic review,” *IEEE Access*, 2024.

[41] A. Steier, L. Ramaswamy, A. Manoel, and A. Haushalter, “Synthetic data privacy metrics,” *arXiv preprint arXiv:2501.03941*, 2025.

[42] T. S. Biró and Z. Néda, “Gintropy: Gini index based generalization of entropy,” *Entropy*, vol. 22, no. 8, p. 879, 2020.

[43] V. Xinying Chen and J. N. Hooker, “A guide to formulating fairness in an optimization model,” *Annals of Operations Research*, vol. 326, no. 1, pp. 581–619, 2023.

[44] J. Chen, Y. Zhang, B. Wang, W. X. Zhao, J.-R. Wen, and W. Chen, “Unveiling the flaws: exploring imperfections in synthetic data and mitigation strategies for large language models,” *arXiv preprint arXiv:2406.12397*, 2024.

- [45] M. Goyal and Q. H. Mahmoud, "A systematic review of synthetic data generation techniques using generative ai," *Electronics*, vol. 13, no. 17, p. 3509, 2024.
- [46] C. Xu, S. Guan, D. Greene, M. Kechadi *et al.*, "Benchmark data contamination of large language models: A survey," *arXiv preprint arXiv:2406.04244*, 2024.
- [47] B. Ronval, P. Dupont, and S. Nijssen, "Detection of large language model contamination with tabular data," in *International Symposium on Intelligent Data Analysis*. Springer, 2025, pp. 234–245.
- [48] S. Bordt, H. Nori, V. Rodrigues, B. Nushi, and R. Caruana, "Elephants never forget: Memorization and learning of tabular data in large language models," in *Conference on Language Modeling (COLM)*, 2024.
- [49] T. Chen and C. Guestrin, "Xgboost: A scalable tree boosting system," in *Proceedings of the 22nd ACM SIGKDD international conference on knowledge discovery and data mining*, 2016, pp. 785–794.
- [50] J. Xu, H. Fei, L. Pan, Q. Liu, M.-L. Lee, and W. Hsu, "Faithful logical reasoning via symbolic chain-of-thought," in *The 62nd Annual Meeting of the Association for Computational Linguistics*, 2024. [Online]. Available: <https://arxiv.org/abs/2405.18357>
- [51] J. Wei, X. Wang, D. Schuurmans, M. Bosma, F. Xia, E. Chi, Q. V. Le, D. Zhou *et al.*, "Chain-of-thought prompting elicits reasoning in large language models," *Advances in neural information processing systems*, vol. 35, pp. 24,824–24,837, 2022.
- [52] S. Mussard, F. Seyte, and M. Terraza, "Decomposition of gini and the generalized entropy inequality measures," *Economics Bulletin*, vol. 4, no. 7, pp. 1–6, 2003.